

## Control and Optimization of Current Profile under Dominant Electron Heating in HL-2A<sup>1</sup>

Qingdi Gao 1), Yongxing Long 1), R. V. Budny 2), Yiming Jiao 1), Xuanton Ding 1), Yudong Pan 1), K. Indreshkumar 2)

1) Southwestern Institute of Physics, Chengdu, Sichuan, P. R. China

2) Princeton Plasma Physics Laboratory, Princeton University, Princeton, NJ, USA

e-mail contact of main author: [qgao@swip.ac.cn](mailto:qgao@swip.ac.cn)

**Abstract.** Establishment of the current profile like in the hybrid scenario is studied under the condition of dominant electron heating in HL-2A. In the discharge of  $q_a \sim 3.4$  a sawtooth-free period was produced following the pellet injection. The discharge is analysed with TRANSP. It is shown that a  $q$ -profile of weak negative shear is produced immediately after the pellet injection, and it then evolves to a broad flat profile with  $q(0) > 0$ . The measured MHD mode structures evidence consistencies of the evaluated  $q$ -profile with the locations of  $q=1$  and  $q=2$  surfaces in the sawtooth period and  $q=2$  surface in the sawtooth-free period. Both the diamagnetic measurement and TRANSP analysis indicate that the energy confinement is enhanced substantially after pellet injection, which would be resulted from the  $q$ -profile optimization. The discharges with injecting LH and EC waves are simulated with TRANSP. Carefully adjusting the position of non-inductive current driven by two groups of gyrotron (each consisting of 2 gyrotrons), an optimized  $q$ -profile was obtained with  $q(a)=3.78$  and low shear region extending to  $x \sim 0.45$  in the low-density discharges (line averaged density  $= 1.0 \times 10^{19} m^{-3}$ ). When 0.5 MW LH power in CD mode and 0.9MW EC power mainly for plasma heating are used to control the current profile, a hybrid discharge scenario with the weak magnetic shear region extending to  $x=0.6$  and  $q(a)=3.21$  is established through controlling the EC absorption position in the low-density plasma ( $1.0 \times 10^{19} m^{-3}$ ). As the constraint imposed by the wave propagation condition in HL-2A limits the maximum allowed  $n_{||}$  - upshift, the LH wave absorption is bounded in the region defined by the strong Landau-damping limit and the boundary of wave propagation domain. This mechanism of the LH wave absorption causes interplay of the distribution of the LH driven current with the modification of the plasma configuration, which constitutes non-linearity in the LH wave deposition. The LH wave deposition position changes spontaneously because of the non-linearity. Therefore, the feedback control of the plasma current profile through controlling the LH driven current is a challenge in the regimes for steady state high performance operation.

### 1. Introduction

Control and optimization of the plasma current profile is a key point in enhancing the plasma performance. Although several tools have been identified that modify transport directly, the effect of the current profile on transport is large and remains an important transport control feature. In tokamak experiments it is demonstrated that the configuration with flat  $q$ -profile in the central plasma region is beneficial to improving plasma confinement. Discharges with internal transport barrier (ITB) have been established with optimized magnetic shear (OS) in JET [1] and ASDEX Upgrade [2], and the developed ITB in this configuration improved central plasma confinement. Recently, so called hybrid scenarios

---

<sup>1</sup>This work is supported by the National Natural Science Foundation of China under grant No. 10275018

characterized by a current density profile, enclosing a large volume of low magnetic shear with  $q_0$  near 1, have achieved improved confinement and higher beta limits [3-6].

The HL-2A tokamak is a divertor tokamak at SWIP (Southwestern institute of Physics), Chengdu, China, with main parameters of major radius  $R=1.64\text{m}$ , minor radius  $a=0.4\text{m}$  toroidal magnetic field  $B_T=2.8\text{T}$ , and plasma current  $I_p=0.48\text{MA}$ . In HL-2A, the various schemes of auxiliary heating and current drive including neutral beam injection (NBI) (2MW), LHCD (1MW) and ECRH (2MW) combined with the device flexibility offer opportunity to optimize the current profile. A single-null divertor (SND) configuration had been established in recent discharges [7,8]. In order to raise the plasma parameters and achieve more interesting operation scenarios, optimization of the plasma configuration will be carried out using the available auxiliary heating schemes. To know the prospective operation scenario, here, establishment of the configuration with central weak magnetic shear is investigated under the current profile control by RF power. Pellet injection has been used to produce high density plasma in HL-2A. In many tokamaks improved energy confinement has been observed with central pellet injection. Analysis of the pellet enhanced performance (PEP) showed that weak or reversed magnetic shear was important in causing the transport reduction. In HL-2A, the pellet injection experiment produced high peaked density plasma with hollow electron temperature profile, and the plasma confinement is improved. In the absence of an MSE measurement, in order to know the current profile modification caused by the pellet injection the experiment is analyzed with TRANSP.

## 2. TRANSP analysis of current profile in the enhanced performance discharge induced by pellet injection

The pellet injection discharge (shot 4050) is shown in Fig. 1. The parameters of the Ohmic heating plasma before pellet injection are:  $I_p=347\text{kA}$ ,  $B_T=2.4\text{T}$ ,  $T_e(0)=1.1\text{keV}$ , and line averaged density  $\bar{n}_e=2.6\times 10^{19}\text{m}^{-3}$ , hydrogen gas. Three hydrogen pellets, of which everyone is of around  $6\times 10^{19}$  atoms, were injected into the plasma successively starting at  $t=0.61\text{s}$  with interval of 55ms between 2 pellets. The pellet speed is about 750m/s. The line

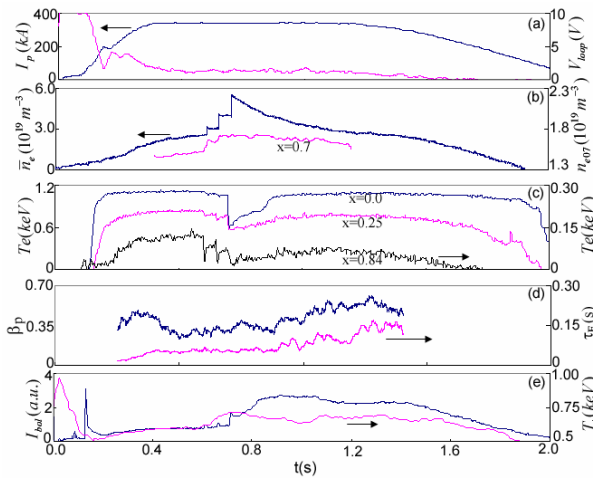


FIG. 1 Temporary evolution of (a)  $I_p$  and loop voltage, (b) line averaged electron density and electron density at  $x=0.7$ , (c)  $T_e$  at  $x=0, 0.25, 0.85$ , (d)  $\beta_p$  and  $\tau_E$ , (e) plasma radiation and  $T_e$ .

average electron density and the density profile are measured with a one-channel HCN laser interferometer and a microwave reflectometry with the scanning frequency range from 24GHz to 50GHz. After the first pellet injection, which increased density mainly at the outer plasma region ( $x>0.6$ ), the last two pellets penetrated into the plasma center, ramping the line average density up to  $\bar{n}_e=5.5\times 10^{19}\text{m}^{-3}$  (Fig. 1). As shown in Fig. 2 the electron density profile is extremely peaked after injection of the total three pellets, since the last pellet penetrates deeply into the plasma center. The very peaked density caused strong central radiation, the profile of which was

measured by the bolometer array. Due to the strong central radiation the electron temperature profile, measured by ECE, became hollow at  $t=0.72\text{s}$ , and it evolved gradually towards flat in the central region until  $t=0.92\text{s}$  (Fig. 3).

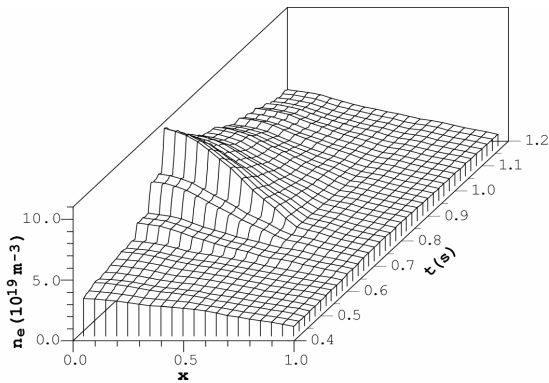


FIG. 2 Temporary evolution of the electron density profile

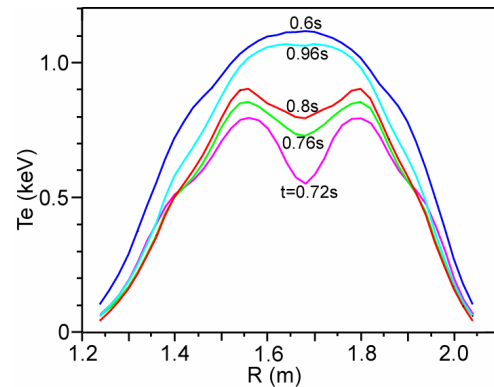


FIG. 3 Electron temperature versus major radius  $R$  at various times.

The discharge is analyzed with TRANSP, and in the analysis neoclassical conductivity is used for the current diffusion. It is shown that a  $q$ -profile of weak negative shear is formed with  $q_0=1.2$  and  $q_{\min}=1.08$  (at  $x_{\min}=0.25$ ) at the end of pellet injection (Fig.4). Following the density profile relaxation after the pellet injection the safety factor distribution evolves towards a broad flat profile, and the plasma configuration with weak magnetic shear extended to  $x\sim 0.4$  is obtained (Fig. 4). The evolution of the plasma current profile is closely correlated with that of the  $T_e$  profile as expected for a Ohmic heating discharge without non-inductive current drive. In addition to  $T_e$ , neoclassical conductivity is dependent on  $Z_{\text{eff}}$  and  $n_e$  as well. Taken into account the uncertainty of the measurement for  $Z_{\text{eff}}$  and the  $n_e$  profile, variations of  $Z_{\text{eff}}$  and the  $n_e$  peaking factor up to  $>30\%$  have been performed in the TRANSP analysis, showing the basic characteristics of  $q$ -profile not changed except some finer modifications to it. The measured MHD mode structures evidence consistencies of the evaluated  $q$ -profile with the experiment measurement. The MHD oscillations measured by soft x-ray arrays show that typical sawtooth precursor of  $m/n=1/1$  mode can be found on sawteeth before pellet injection. It is estimated that the reversed radius of sawteeth is at  $x\sim 0.14$ , which is in

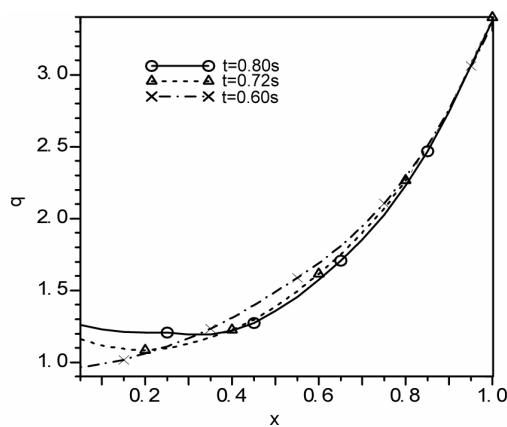


FIG. 4  $q$ -profiles before (at  $t=0.6\text{s}$ ), and after pellet injection (at  $t=0.72, 0.8\text{s}$ )

reasonable agreement with the calculated  $q=1$  surface position at  $x=0.12$ . After the pellet injection, sawtooth disappears for a period of  $\sim 140\text{ms}$ . The calculated period of  $q_0 > 1$  is over  $200\text{ms}$  that is longer than the measured sawtooth-free period. This disagreement is possibly caused by the effect of anomalous Ohmic current diffusion. Furthermore, the mode structure analysis from the low frequency MHD oscillations ( $\sim 3\text{kHz}$ ), which can be observed by soft x-ray detectors and Mirnov probes, shows that the location of  $q=2$  surface is roughly in agreement with the calculated  $q=2$  position (at  $x=0.75$ ) after pellet injection [9].

Both the diamagnetic measurement and TRANSP analysis indicate that the energy confinement is enhanced substantially after pellet injection. This would be resulted from the  $q$ -profile optimization in addition to the density peaking.

### 3. Simulation of current profile control with RF wave injection

The above produced current density profile of low magnetic shear is transient and not controllable. In order to establish stationary optimized  $q$ -profile, RF waves will be applied in HL-2A to control the current density profile. HL-2A has two different RF systems at different frequency ranges: lower hybrid (LH) wave at frequency of 2.45GHz and electron cyclotron (EC) wave at frequency of 68GHz. The LH power is generated with 2 klystrons of 0.5MW each and radiated by a multi-junction (2×12) antenna. The EC power is generated by 4 gyrotrons with 0.5MW each, and direction of the radiated EC beams can be varied toroidally and poloidally by rotating the steerable mirrors. Both of the heating schemes heat electrons directly producing hot electron plasmas. They are proved to be effective current drivers as well. Their driven current profiles were studied in detail. To know the prospective operation scenario upon the current profile control, the discharges with injecting LH and EC waves are simulated with TRANSP. The propagation and absorption of LH wave is calculated by LSC and that of EC wave is calculated by TORAY. The plasma of single-null divertor ( $\delta_L=0.25$ ,  $k\sim 1.0$ ) obtained in the previous experiment [7] is used in the simulation. The geometry of the boundary (99.8% flux surface of the diverted plasma) is specified as a general function of time, which evolves from circular to SDN shape during the current ramping-up phase and then keeping the same shaped boundary in the current flattop phase. The interior flux surfaces, which are computed by solving the Grad-Shafranov equation, are parameterized by the square-root of the normalized toroidal flux  $\rho$ . The energy transport model is a mixed theory model in which the ion heat diffusivity is assumed in terms of neoclassical transport enhanced by  $\eta_i$  turbulence, and the electron energy transport is based on the Rebut-Lallia-Watkins (RLW) model.

**Profile control with EC wave.** We first investigate the current profile optimization by carefully adjusting the position of non-inductive current driven by two groups of gyrotrons (each consisting of 2 gyrotrons). As a dimensionless parameter  $\beta_N H/q_{95}^2$  is considered to be the figure of merit for evaluating the hybrid scenarios, the criterion for the optimization is set to be that the volume of weak magnetic shear with  $q_0\approx 1$  is as large as possible and the edge  $q$  ( $q_a$ ) as low as possible. The target plasma is a Ohmic heating plasma with  $I_p = 340\text{kA}$ ,  $B_T = 2.43\text{T}$ , and  $\bar{n}_e = 1.0 \times 10^{19} \text{ m}^{-3}$ . In order to drive non-inductive current to control the current profile the EC wave is lunched toroidally at an azimuthal angle of  $200^\circ$ . The driven current position is controlled by the polar lunched angle. Since ECCD drives spatially localized current in a smaller scale, the EC waves from different gyrotrons are lunched at different polar angles of  $82.9^\circ$ ,  $79.9^\circ$  and  $2 \times 77.9^\circ$  respectively to produce broad EC power deposition (Fig. 5b). With  $2 \times 0.95\text{MW}$  EC power injected at  $t=0.6\text{s}$ , the central  $q$  gradually increases to  $q_0 \geq 1.0$  at  $t \approx 0.9\text{s}$  producing a configuration of weak magnetic shear. In this configuration the low shear region extends to  $x \sim 0.45$  with  $q_0 \geq 1.0$ ,  $q_a = 3.73$  (Fig. 5a), and it is steadily maintained until the EC power is taken off at  $t=1.4\text{s}$ . Corresponding to the optimized  $q$  profile an ITB is developed (at  $x \sim 0.45$ ) on the electron temperature profile, showing that this is an OS configuration. It is interesting to notice that when the OS configuration is not formed at the

early time of ECCD (e. g.  $t=0.65s$ ), the ITB on the temperature profile is not developed either as shown by the purple lines in Fig.5. The correlation between the current profile optimization and the confinement improvement shows consistency of the transport simulation.

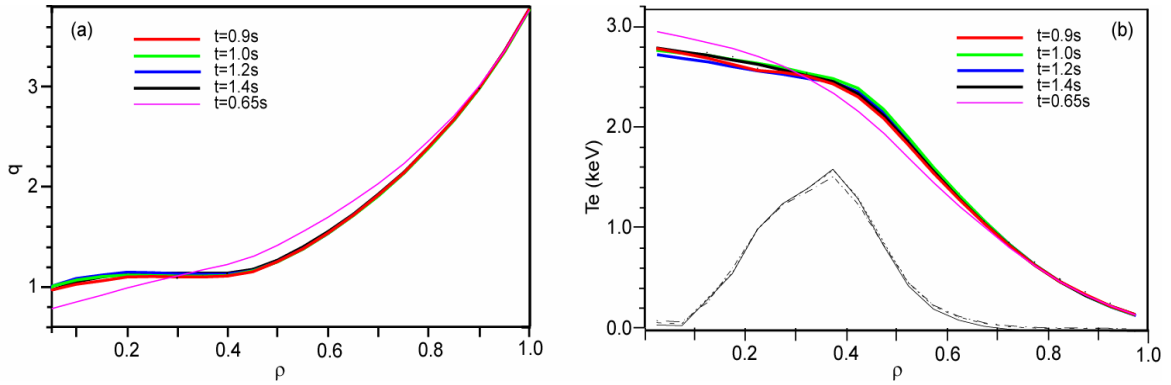


FIG. 5 (a)  $q$ -profiles, and (b)  $T_e$ -profiles at different times during ECCD, purple lines being profiles at early time when the OS configuration is not formed. Black lines in (b) indicate the EC power.

Although ECCD has its strong controllability of local current density, its efficiency is strongly dependent on  $T_e$  and rather low. As we try to extend the weak shear region broader by moving the EC power deposition outside, the EC driven current is too low to maintain the optimized magnetic shear. Similarly, if we reduce  $q_a$  by increasing the plasma current, the fraction of non-inductive current driven by EC, which is  $I_{EC} \sim 60kA$  in the above case, is not enough to elevate the central  $q$  to  $q_0 \geq 1.0$ . It is also due to the rather low non-inductive driven current by EC that the OS configuration is not able to be formed when the plasma density is higher.

**Profile control by ECH+LHCD.** Considering the advantages of the LH scheme that drives current efficiently, we employ LHCD for large-scale  $q(r)$  control. To compare with the ECCD controlled scenario above, here a low-density plasma of  $\bar{n}_e = 1.0 \times 10^{19} m^{-3}$  and  $I_p = 400kA$ ,  $B_T = 2.43T$  is considered. The target plasma is heated by EC of  $0.48MW + 0.47MW$  lunched from 2 gyrotrons. By adjusting the polar lunched angle the EC power from 2 gyrotrons deposits around  $\rho = 0.2$  and  $\rho = 0.3$  respectively. From the evolution of  $q$  at various locations (Fig. 6), it is shown that the  $q$ -profile has a little change in the ECH phase. To control the current profile,  $0.5 MW$  LH power in the current drive mode (the multi-junction antenna phasing  $\Delta\phi=90^\circ$ ) is injected. As the LH wave deposition primarily governed by a nonlinearity

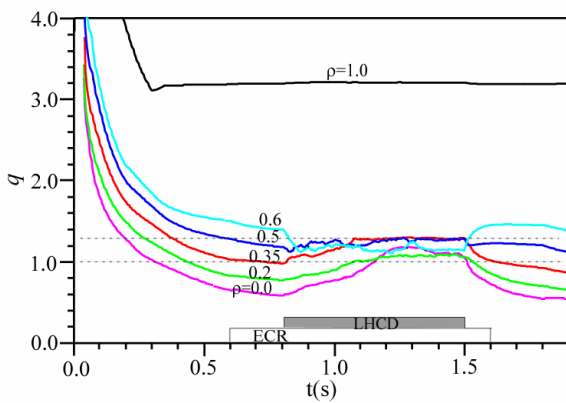


FIG. 6 Temporary evolution of  $q$  at various flux surfaces.

between the deposition profile and the electron temperature profile, the  $q$ -profile adjusts slowly, and the safety factor between  $\rho=0.0$  and  $\rho=0.7$  evolves gradually to the new value on the resistive time scale. After the current profile is fully relaxed, the  $q$  values of  $\rho = 0.0-0.6$  constrict to a narrow range of  $1.0-1.3$  (Fig. 6), and a  $q$ -profile with weak shear region extended to  $x=0.6$  and  $q_a=3.21$  (Fig. 7a) is established. It is sustained until LHCD is turned off. Though the  $q$ -profile in the weak shear region is not as flat as that in

the discharge controlled by ECCD, the absolute value of the magnetic shear  $s[\equiv(dq/dr)\times(r/q)]$  is rather low (Fig. 7b). Compared to the EC-only control scheme, the current profile control with the combination of EC and LH is more flexible and more efficient. In the ECH+LHCD scenario, the EC wave, which heats the plasma efficiently, increases the electron temperature in the central region, which makes the LH wave penetrating deeply into the plasma to drive current in a wider region. It is due to the wider region for the LH current driving and the much higher current drive efficiency of LHCD that the central flat  $q$ -profile with wider region and lower edge  $q$  value can be formed, and the discharge has achieved fully non-inductive current drive. With the similar control scheme the  $q$ -profile with the weak magnetic shear region extended to  $\rho=0.45$  and  $q_a=3.36$  has been produced in a higher density plasma of  $\bar{n}_e=2.32\times 10^{19}m^{-3}$ .

As shown in Fig. 7(c) the electron temperature profile does not show a change corresponding to the optimized current profile as is often the case with an electron-ITB developed (see the EC-only scenario above). However, the electron temperature increases

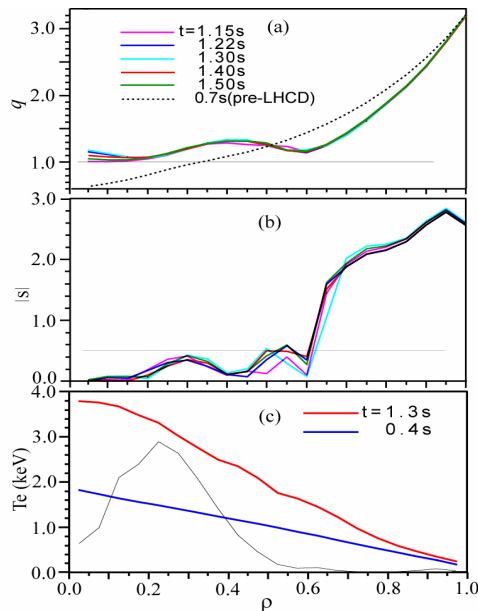


FIG. 7 (a)  $q$ -profiles, and (b) absolute value of magnetic shear versus  $\rho$  at various times, (c)  $T_e$ -profiles at  $t=0.4s$  (Ohmic phase), and  $t=1.3s$ , thin black line indicating electron heating power.

largely, and its normalized gradient  $R/L_T$  (where  $1/L_T = \nabla T_e/T_e$ ) becomes larger than the critical gradient value ( $R/L_T < 10$ ) for temperature profile stiffness [10] in the confinement region of  $\rho < 0.8$ , characteristic of the suppression of the electron temperature gradient (ETG) and/or trapped electron mode (TEM) driven turbulences. The characteristics of the plasma confinement indicate a hybrid discharge scenario established by controlling the plasma profile with both ECH and LHCD. The transport of the NBI heated hybrid discharges in DIII-D have been simulated with GLF23 model. The GLF23 model [11] is a gyrofluid representation of the transport due to ITG (ion temperature gradient), TEM and ETG modes and can optionally include the effect of  $\mathbf{E}\times\mathbf{B}$  on shear on the mode spectrum and associated transport. Modelling of this class of discharges indicates that inclusion of  $\mathbf{E}\times\mathbf{B}$  shear stabilization is an important ingredient in reproducing the measured temperature profiles. While this is suggestive that  $\mathbf{E}\times\mathbf{B}$  shear stabilization is important in these discharges, it is unclear whether the improved confinement is due to large levels of  $\mathbf{E}\times\mathbf{B}$  shear or reduced turbulence drive associated with a favourable current profile with low magnetic shear. The hybrid discharges established by the RF-only control scheme should be helpful to distinguish these mechanisms for the confinement improvement.

#### 4. Non-linearity effects of the LH wave power deposition

Though the LH wave has the advantage of quite high CD efficiency, its absorption in the HL-2A plasma is weak and it makes many passes through the plasma until the initial launched wave spectrum is sufficiently broadened to be absorbed. As the constraint imposed

by the wave propagation condition limits the maximum allowed  $n_{//}$  - upshift, the LH wave absorption is bounded in the region defined by the strong Landau-damping limit and the boundary of wave propagation domain. **At the boundary of the propagation domain,**

$$\bar{n}_{//} = n_{//0} \frac{R_0}{R} \frac{\hat{q}^2 \mp \sqrt{1 + (1 + \hat{q}^2)(\omega_{pe}^2 / \omega^2) / \varepsilon_{\perp}}}{\hat{q}^2 - [1 + (\omega_{pe}^2 / \omega^2) / \varepsilon_{\perp}]}, \quad (1)$$

where  $n_{//0}$  and  $R_0$  refer to the toroidal mode number  $n$  launched at the antenna  $R_0$ ,  $\hat{q} = q_{cyl} / \varepsilon$

( $q_{cyl}$  is the cylindrical safety factor,  $x=r/a$ , and  $\varepsilon=a/R$ ) is a magnetic geometry factor, and

$\varepsilon_{\perp} = 1 + \omega_{pe}^2 / \omega_{ce}^2 - \sum_j \omega_{pi,j}^2 / \omega^2$ . To achieve LH wave power deposition in the weak

damping regime, we rely on the  $n_{//}$  - upshift to fill the spectrum gap. The limit of the  $n_{//}$  - upshift is defined by

$$n_{//} \leq n_{//0} \frac{R_0 / R}{1 - (\omega_{pe} / \omega) / (\hat{q} \varepsilon_{\perp}^{1/2})}. \quad (2)$$

Strong Landau damping requires condition of

$$n_{//} = k_{//} c / \omega \geq 6.5 / \sqrt{T_e [Kev]}. \quad (3)$$

The region defined by strong electron Landau damping and the boundary of wave propagation domain is related to the distribution of plasma parameters, especially, the wave propagation domain is dependent explicitly on the safety factor profile. Accordingly the LH power deposition position depends on both the current and pressure profiles. As the current density profile changed due to LHCD, both the current profile and pressure profile are modified, in turn affecting the LHCD location again. The interplay of the LHCD location with the modification of the plasma configuration constitutes non-linearity in the LH wave deposition [12]. In the tokamak operation, to control the LHCD position through adjusting the radiated power spectrum is a feasible way for feedback control. By using the control with

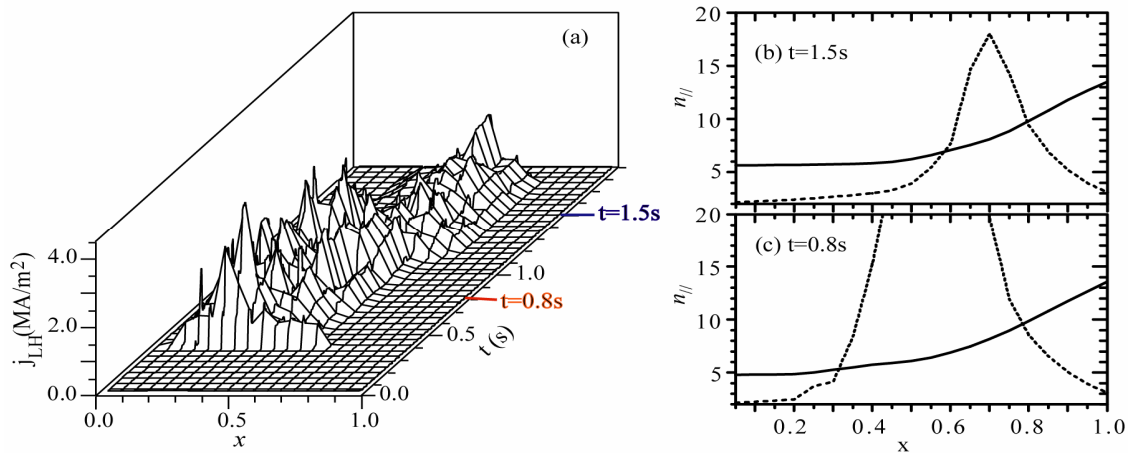


FIG. 8 (a) Temporal evolution of LH wave driven current profile for the case of the LH spectrum produced with  $\Delta\phi = 75^\circ$ . LH power absorption region in the phasing space ( $x, n_{//}$ ) defined by electron Landau damping limit (full line), and boundary of the wave propagation domain (dotted line) (b) at  $t=1.5s$ , (c) at  $t=0.8s$ .

LHCD of  $\Delta\phi = 90^\circ$ , a stable reversed magnetic shear (RS) plasma has been established [13]. However, as we change the radiated LH spectrum by changing the antenna phasing to  $\Delta\phi = 75^\circ$ , the location of the LH wave driven current changes spontaneously, generating two distinct quasi-stationary RS in a single discharge without changing the discharge condition (Fig. 8). Therefore, the feedback control of the plasma current profile through controlling the externally driven current by the LH wave is a challenge in the steady state high performance tokamak operation.

## 5. Conclusions

In HL-2A, pellet injection produces high peaked density plasmas with hollow electron temperature profile. The TRANSP analysis of the experiment shows that a  $q$ -profile of weak negative shear is formed following the pellet injection, and it then evolves to a broad flat profile with the weak magnetic shear region extended to  $x=0.4$ . The enhanced plasma performance induced by pellet injection could be related to the current profile modification.

The predictive simulation of current profile control with the available RF heating schemes in HL-2A demonstrates that the optimized  $q$ -profile with wide weak magnetic shear region can be established by carefully adjusting the EC power deposition. In the EC-only scenario, the optimized  $q$ -profile is established with an ITB developed on the electron temperature profile (electron-ITB). The control scheme of ECH+LHCD is more effective, with which a hybrid configuration with the central weak shear region extended to  $x=0.6$  can be produced.

In the HL-2A plasma the LH wave absorption is bounded in the region defined by the Landau-damping limit and boundary of wave propagation domain. This mechanism causes interplay of the distribution of the LH wave driven current with the modification of the plasma configuration, which constitutes non-linearity in the LH wave deposition. Due to the non-linear effects of the LH power deposition, the LH wave deposition position changes spontaneously. Therefore, the feedback control of the current profile through controlling LHCD is a challenge in the steady state high performance tokamak operation.

## References

- [1] Gormezano, C., et al., Phys. Rev. Lett. 80 (1998) 5544
- [2] Gruber, O., et al., Phys. Rev. Lett. 83 (1999) 1787
- [3] Joffrin, E., et al., Nucl. Fusion 45 (2005) 626
- [4] Wade, M. R., et al., Nucl. Fusion 45 (2005) 407
- [5] Staebler, A., et al., Nucl. Fusion 45 (2005) 617
- [6] Luce, T. C., et al., Nucl. Fusion 43 (2003) 321
- [7] Gao, Q. D., et al., 2004 Proc. 20th Int. Conf. on Fusion Energy (Vilamoura, 2004) (Vienna: IAEA) CD-ROM file EX/P4-21
- [8] Yuan, B. S., et al., 2004 Proc. 20th Int. Conf. on Fusion Energy (Vilamoura, 2004) (Vienna: IAEA) CD-ROM file EX/P5-35
- [9] Ding, X. T., et al., Chin. Phys. Lett. 23 (2006) 1795
- [10] Ryter, F., et al., Plasma Phys. Control. Fusion 43 (2001) A323
- [11] Waltz, R.E., Dewar, R. L., and Garbet, X., Phys. Plasmas 5 (1998) 1784
- [12] Gao, Q. D., Phys. Plasmas 12 (2005) 122507
- [13] Gao, Q. D, et al., Nucl. Fusion 43 (2003) 982